Research Article

Nano Research
2022, 15(3): 2634–2642

ISSN 1998-0124 CN 11-5974/O4
https://doi.org/10.1007/s12274-021-3858-1

Precursor compound enabled formation of aqueous-phase CdSe magic-size clusters at room temperature

Min Zhao[1], Qingyuan Chen[2], Yongcheng Zhu[2], Yuehui Liu[3], Chunchun Zhang[4], Gang Jiang[2], Meng Zhang[2] (✉), and Kui Yu[2,3,5] (✉)

[1] *School of Chemical Engineering, Sichuan University, Chengdu 610065, China*
[2] *Institute of Atomic and Molecular Physics, Sichuan University, Chengdu 610065, China*
[3] *Engineering Research Center in Biomaterials, Sichuan University, Chengdu 610065, China*
[4] *Analytical & Testing Center, Sichuan University, Chengdu 610065, China*
[5] *State Key Laboratory of Polymer Materials Engineering, Sichuan University, Chengdu 610065, China*

Received: 5 July 2021 / **Revised:** 25 August 2021 / **Accepted:** 2 September 2021

ABSTRACT

The formation pathway of aqueous-phase colloidal semiconductor magic-size clusters (MSCs) remains unrevealed. In the present work, we demonstrate, for the first time, a precursor compound (PC)-enabled formation pathway of aqueous-phase CdSe MSCs exhibiting a sharp absorption peaking at about 420 nm (MSC-420). The CdSe MSC-420 is synthesized with $CdCl_2$ and selenourea as the respective Cd and Se sources, and with 3-mercaptopropionic acid or L-cysteine as a ligand. Absorption featureless CdSe PCs form first in the aqueous reaction batches, which transform to MSC-420 in the presence of primary amines. The coordination between primary amine and Cd^{2+} on PCs may be responsible to the PC-to-MSC transformation. Upon increasing the reactant concentrations or decreasing the $CdCl_2$-ligand feed molar ratios, the Cd precursor self-assembles into large aggregates, which may encapsulate the resulting CdSe PCs and inhibit their transformation to MSC-420. The present study sheds essential light on the syntheses and formation mechanisms of nanocrystals.

KEYWORDS

aqueous magic-size cluster, precursor compound, formation pathway, self-assembly, precursor configuration

1 Introduction

Semiconductor magic-size clusters (MSCs) have their counterpart precursor compounds (PCs) [1–20]. The main difference between both is that the MSCs exhibit sharp characteristic absorption peaks but the PCs are generally featureless in optical absorption. In organic-phase metal (M) chalcogenide (E) reaction systems, the ME PCs form first upon the self-assembly and the subsequent covalent bonding of M and E precursors [18]. After incubation or dispersing in certain organic solvents, the resulting PCs then transform to MSCs via intramolecular reorganization [2–19]. The PCs may dissociate to result in fragments that support the nucleation and growth of quantum dots (QDs) [9, 12]. Moreover, one PC is able to interact with monomers/fragments (M/F) in the reaction systems via either substitution or addition reaction to produce a new PC with different structures and/or compositions [2, 3, 7, 9, 11–13, 20]. Such a PC-to-PC transformation is responsible to the apparent transformation among MSCs. It is noteworthy that the semiconductor PCs are quite conceptually similar to the $(CaCO_3)_n$ (n = 3–11) oligomers and Posner molecules $(Ca_3(PO_4)_2)_3$ as intermediates for the formation of calcium-based inorganic nanomaterials [21, 22].

So far, the syntheses of aqueous-phase semiconductor nanoparticles, including QDs and MSCs, are quite empirical [23–36]. The understanding about the reaction mechanism of these synthetic approaches in aqueous solutions remains limited, which is mainly attributed to the complicated ionic environments in aqueous solutions [23, 27]. There are synthetic approaches of aqueous-phase CdSe [31–36] and CdS MSCs [1] that have been reported in literature. The CdSe MSCs are synthesized in water with $CdSO_4$ and Na_2SeSO_3 as the respective Cd and Se sources, and with L-cysteine ($HS–CH_2–CH(NH_2)–COOH$, Cys) as the ligand. CdSe MSCs exhibiting a sharp absorption peak at about 420 nm (denoted as MSC-420 according to the primary absorption peak) form gradually in the reaction batches. However, such an approach suffers from poor stability of the Se source (Na_2SeSO_3) and long reaction durations (about 6–7 days) [31], and the formation mechanism of MSCs is left unrevealed. The CdS MSCs are synthesized with $CdCl_2$ and thiourea as the respective Cd and S sources, and with 3-mercaptopropionic acid ($HS–CH_2–CH_2–COOH$, MPA) as the ligand. Addition of a primary amine, such as butylamine ($CH_3–(CH_2)_3–NH_2$, BTA), into the mixtures promotes the decomposition of thiourea and induces the formation of CdSe MSCs with a characteristic absorption peak at about 360 nm (denoted as MSC-360). The purified CdS MSC-360 transforms to its counterpart PCs after being dispersed in deionized water, while the MSC-360 recovers upon addition of primary amines [1]. In such a reaction system, both the decomposition of thiourea and the formation of MSC-360 occur simultaneously after addition of BTA. Therefore, the

Address correspondence to Meng Zhang, mengzhang@scu.edu.cn; Kui Yu, kuiyu@scu.edu.cn

formation pathway of CdS MSC-360 in aqueous solutions from precursors remains to be explored.

In the present work, we demonstrate the PC-enabled formation pathway of aqueous-phase CdSe MSC-420 at room temperature. The CdSe MSC-420 is synthesized with $CdCl_2$ and selenourea (SeU) as the respective Cd and Se sources, and with MPA as a ligand. SeU is a commercially available compound that may be hydrolyzed in alkaline aqueous solutions. The use of SeU may help to obtain CdSe PCs in aqueous solutions with the absence of primary amines, which facilitates the investigation for the formation pathway of CdSe MSC-420. The reaction mixture of these reactants in an alkaline aqueous solution remains absorption featureless upon incubation, while the addition of a primary amine, such as BTA, promotes the formation of CdSe MSC-420. Electrospray ionization mass spectrometry (ESI-MS) suggests the incubated CdSe solution with absorption featureless forms CdSe PCs. ^{1}H nuclear magnetic resonance (NMR) spectroscopy suggests the coordination of primary amine with Cd^{2+}, which may be responsible to the transformation from the CdSe PCs to MSC-420. The Cd-MPA complexes may self-assemble to large aggregates, which are facilitated upon decreasing the $CdCl_2$-MPA feed molar ratio. The resulting aggregates encapsulate the PCs and inhibit their transformation to MSC-420. When Cys is used as a ligand, MSC-420 evolves in the alkaline aqueous solution without the addition of primary amine. We argue that the formation of CdSe PCs and their transformation to MSC-420 occur simultaneously due to the presence of primary amine group on Cys. With a high $CdCl_2$ to Cys feed molar ratio, the resulting Cd-Cys complex exhibits a partially closed configuration with both thiol and amine groups coordinated with Cd^{2+}. Such a configuration of Cd-Cys complex decreases its reactivity towards the formation of CdSe PCs and MSC-420. With a low $CdCl_2$ to Cys feed molar ratio, the self-assembly of the resulting Cd-Cys complex is facilitated, which inhibits the formation of CdSe MSC-420 as well. The present study demonstrates that the PC-enabled formation pathway model of semiconductor MSCs in organic-phase reaction system is also applicable to the aqueous-phase one, promoting the syntheses of semiconductor nanomaterials from an empirical art to science.

2 Experimental

2.1 Chemicals

SeU (98%), MPA (99%), Cys (97%), BTA (99.5%), pyrene (99%) and deuterium oxide (D_2O, 99%) were purchased from Sigma-Aldrich. $CdCl_2·2.5H_2O$ (99%) was purchased from Chengdu Kelong Chemical. Potassium hydroxide (KOH, 85%) was obtained from Tianjin Zhiyuan Chemical. Propylamine (PrA, 99%) was obtained from Tianjin Guangfu Chemical. Ethylamine aqueous solution (ETA, 70%) was purchased from Alfa Aesar. All the chemicals were used without further purifications.

2.2 Preparation of Cd precursor stock solutions

The Cd precursor stock solutions were prepared upon mixing $CdCl_2·2.5H_2O$ (23 mg, 0.10 mmol) with either MPA (35 μL, 0.40 mmol) or Cys (49 mg, 0.40 mmol) in 5.00 mL deionized water under stirring. To the resulting aqueous solution, KOH solution (1.00 M) was used to adjust the pH to a certain value. Subsequently, deionized water was added to obtain a mixture with a total volume of 10.00 mL, and the resulting solutions were kept under ambient conditions for further usage.

2.3 Synthesis of CdSe MSC-420

2.3.1 Synthesis of CdSe MSC-420 with MPA as the ligand

In the Cd precursor stock solution (10.00 mL) with MPA, SeU (6 mg, 0.05 mmol) was added at room temperature under stirring. Aliquots of the as-mixed sample or the sample with an incubation for 3 h were extracted and dispersed in a mixture of BTA and deionized water. The resulting sample with BTA was then kept at room temperature for various durations towards the formation of CdSe MSC-420.

2.3.2 Synthesis of CdSe MSC-420 with Cys as the ligand

In the Cd precursor stock solution (10.00 mL) with Cys, SeU (6 mg, 0.05 mmol) was added at room temperature under stirring. The resulting aqueous sample was then kept at room temperature for various durations towards the production of CdSe MSC-420.

2.4 Characterization

2.4.1 Absorption spectroscopy

Optical absorption spectra were collected with an interval of 1 nm on TECHCOMP UV 2310 II ultraviolet–visible (UV–vis) spectrometers. Background measurements were performed with deionized water.

2.4.2 Fluorescence spectroscopy

A stock solution of pyrene (0.3 μM) was used throughout the fluorescence measurements. The samples were prepared in the pyrene stock solution with various ratios of $CdCl_2$ to either MPA or Cys with different $CdCl_2$ concentrations. KOH was added with 2.5 times concentrations as high as that of MPA or Cys to result in an alkaline environment. The solutions were kept for 24 h at room temperature before fluorescence measurements. The emission spectra were collected on Horiba Fluoromax-4 spectrometer with an excitation wavelength of 335 nm, and with the excitation and emission slit widths of 2.5 nm.

2.4.3 ^{1}H NMR and heteronuclear single quantum coherence (HSQC) spectroscopy

The solutions were prepared in deuterium oxide (D_2O). All the spectra were collected on Bruker A II 400 MHz spectrometer.

2.4.4 ESI-MS

The ESI-MS measurements were performed with an Agilent 6210A HPLC-TOF/MS in a positive ion mode. Acetonitrile was used as a mobile phase. Agilent Mass Hunter software was used for the collection and analysis of ESI-MS spectra.

2.4.5 Computation

All density functional theory (DFT) calculations were carried out via Gaussian software under the M062X/Def2-TZVP level [37]. The polarized continuum model (PCM-SMD) [38, 39] of water was considered to simulate the solvent effect. Frequency calculations were performed to evaluate the stabilities of structures and to obtain the Gibbs free energy.

3 Results and discussion

3.1 Evolution of CdSe MSC-420 with MPA as the ligand

Figure 1 presents the optical absorption spectra of CdSe reaction batches ((a)–(c)) and of SeU aqueous solutions ((d)–(f)). For the CdSe reaction batches, an aqueous sample (pH about 12.0) with a feed molar ratio of $2CdCl_2$-8MPA-1SeU and with a $CdCl_2$ concentration of 10.0 mM was prepared first. An aliquot (60 μL)

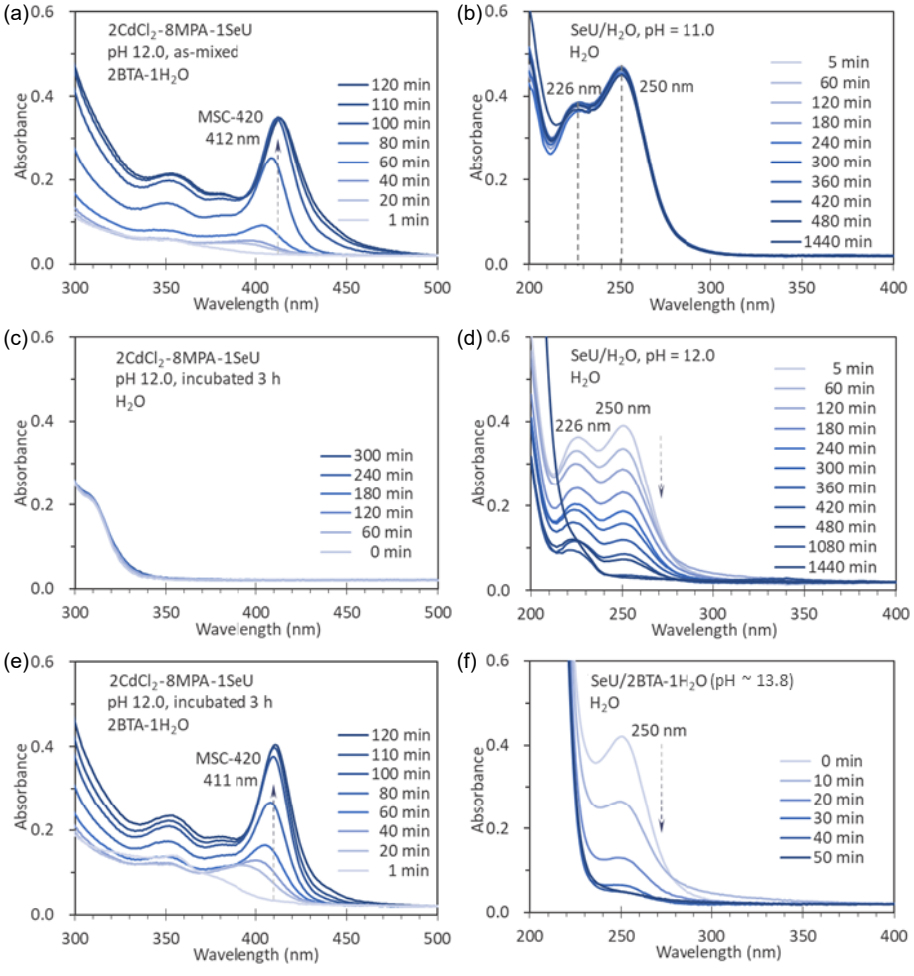

Figure 1 Investigations of the formation of aqueous-phase CdSe MSC-420 and the hydrolysis of SeU. An aqueous sample of $2CdCl_2$-8MPA-1SeU was prepared first with a $CdCl_2$ concentration of 10.0 mM. The as-mixed sample was extracted and dispersed in a mixture of BTA and water (a). After an incubation period of 3 h, the incubated aqueous sample was extracted and dispersed in either water (b) or a mixture of BTA and water (c). The absorption spectra were collected for each solution after certain durations as indicated. SeU stock solutions with a concentration of 5.0 mM were prepared first in aqueous solutions with pH of 11.0 (d) and 12.0 (e), or in a mixture of BTA and water (f). After certain periods as indicated, each SeU stock solution was extracted and dispersed in water for absorption measurement. The formation of MSC-420 obtained in the BTA-water mixture from the incubated sample is faster than that from the as-mixed one, which may suggest the formation of absorption featureless CdSe PCs in the incubated aqueous sample.

of the as-mixed aqueous sample was dispersed in a mixture of BTA (2.00 mL) and water (0.94 mL) (a), and the same volume of the incubated sample was dispersed in either water (2.94 mL) (b) or a mixture of BTA (2.00 mL) and water (0.94 mL) (c). Absorption spectra of each sample were collected after various durations as indicated. For the SeU aqueous solutions, stock aqueous solutions of 5.0 mM SeU were prepared in water with pH values of 11.0 (d) and 12.0 (e), and in a mixture of BTA (2.00 mL) and water (1.00 mL) (f). After certain reaction periods, an aliquot (30 μL) of each SeU stock solution was extracted and dispersed in water (2.97 mL) for absorption measurement.

When the as-mixed $2CdCl_2$-8MPA-1SeU aqueous sample was dispersed in the BTA-water mixture, a primary peak at about 350 nm with an absorbance of about 0.06 appeared after about 1 min. The peak shifted to about 393 nm with an absorbance of 0.05 after reacting for 20 min. Subsequently, the peak redshifted gradually over time, with the absorbance increasing simultaneously. After 100 min, the peak appeared at 412 nm with an absorbance of about 0.35, which changed little in the following 20 min (Fig. 1(a)). When the incubated $2CdCl_2$-8MPA-1SeU aqueous sample was dispersed in water, the resulting solution displayed no obvious characteristic absorption peak and changed little up to 300 min (Fig. 1(b)). Upon dispersing the incubated $CdCl_2$-8MPA-1SeU aqueous sample in the BTA-water mixture, the primary absorption peak located at 380 nm with an absorbance of 0.08 after reacting for 1 min. Similarly, the peak redshifted and increased in absorbance gradually over time. After 110 min, the peak was at 411 nm with an absorbance of 0.40, which changed little in the following 10 min (Fig. 1(c)).

The SeU exhibits a characteristic absorption peak at about 250 nm in aqueous solutions. We noticed that in an aqueous solution with a pH of about 11.0, the absorption peak of SeU changed little in durations up to 1,440 min (Fig. 1(d)), suggesting that SeU remained stable under such conditions. When the pH value increased to about 12.0, the absorption peak of SeU, however, decreased in intensity gradually over time, and almost disappeared after 1,080 min (Fig. 1(e)). In a mixture of BTA (2.00 mL) and water (1.00 mL), the absorption peak of SeU almost disappeared in about 40 min (Fig. 1(f)). These results suggest the hydrolysis of SeU in aqueous solutions under a high pH or in the presence of BTA. Upon increasing the pH (Fig. S1 in the Electronic Supplementary Material (ESM)) or the volume of BTA in the aqueous solutions (Fig. S2 in the ESM), the hydrolysis of SeU was facilitated significantly. By increasing the volume of BTA from 0.5 to 2.0 mL in the BTA-water mixtures with a total volume of 3.0 mL, the pH of the resulting BTA-water mixtures increased from 12.5 to 13.8 (Fig. 1(f) and Fig. S2 in the ESM), which may lead to the fast hydrolysis of SeU. We noticed that upon the hydrolysis of SeU, the SeU aqueous solutions evolved from transparent to turbid with a color of brown, resulting in black precipitates eventually.

The appearance of the characteristic absorption peak shown in Fig. 1(a) suggests the formation of CdSe MSC-420 in the absence of CdSe QDs from the as-mixed sample in the BTA-water mixture due to the BTA-promoted hydrolysis of SeU. The incubated aqueous sample remained absorption featureless in water, but displayed the formation of MSC-420 in the BTA-water mixture. It worth noting that the intensity of MSC-420 absorption peak obtained from the incubated sample remained higher than that obtained from the as-mixed sample in the same reaction period in BTA-water mixture (Fig. S3 in the ESM). Therefore, we argue that the absorption featureless CdSe PCs formed in the incubated aqueous sample (Fig. 1(b)), which is supported by the hydrolysis of SeU in aqueous solutions with a pH of about 12.0. The resulting PCs then transform to CdSe MSC-420 in the presence of BTA (Fig. 1(c)). Upon dispersing the as-mixed sample in the BTA-water mixture, the formation of CdSe PCs and their transformation to CdSe MSC-420 occurred simultaneously (Fig. 1(a)). Nevertheless, a quantitative analysis of the conversion kinetics from CdSe PCs to MSC-420 remains challenging, even for the incubated sample. It is difficult to purify CdSe PCs from the incubated sample, while addition of BTA into the incubated sample promotes the hydrolysis of unreacted SeU towards the formation of new CdSe PCs. Therefore, we are not able to obtain a simple PC to MSC transformation process for further analysis.

The CdSe PCs formed are supposed to be amorphous [6], and exhibit similar molecular mass of the inorganic core with that of MSC-420 [17]. We argue that the PC-to-MSC transformation in the presence of BTA may involve the variation of surface passivation for the CdSe PCs. It is noteworthy that the excess Cd-MPA complexes in the reaction system may surround in the adsorption layer of CdSe PCs and MSCs to protect them from oxidation by dissolved O_2 [40]. Similar PC-to-MSC transformations in the presence of a primary amine (BTA or octylamine) were also observed in nonaqueous reaction systems regarding CdSe [16], CdTe [5, 13, 14], CdTeSe [7], and ZnSe [15] MSCs. When the $CdCl_2$-8MPA-1SeU aqueous sample was incubated for a long period such as 27 or 72 h (Fig. S4 in the ESM), the resulting CdSe PCs seem to transform to a species with an absorption peak at about 350 nm. The resulting species with a long incubation period seems to be a CdSe coordination polymer that is a fibrillar intermediate with a characteristic absorption peak at about 350 nm [41, 42].

Besides BTA, the use of other primary amines, such as PrA and ETA (70% aqueous solution), were also able to promote the formation of CdSe MSC-420 from either as-mixed (Fig. S5 in the ESM) or incubated samples (Fig. S6 in the ESM). Increasing the volume of primary amine up to 2.0 mL in a 3.00 mL amine-water mixture seemed to facilitate the evolution of MSC-420, resulting in a faster formation rate and a sharper characteristic absorption peak. However, further increase of the volume of PrA and BTA to about 3.0 mL seemed to suppress the formation of MSC-420 due to the precipitation of reactants (Figs S5(b4), S5(c4), S6(b4) and S6(c4) in the ESM), while using about 3.0 mL ETA resulted in the evolution of MSC-420 with the co-existence of a new species peaking at 437 nm (Figs. S5(a4) and S6(a4) in the ESM).

3.2 The detection of CdSe PCs via ESI-MS

ESI-MS has been widely employed to investigate the formation of PCs in the induction period samples [11, 16, 18]. Figure 2(a) presents the ESI-MS spectra for an as-mixed sample (trace (1)), and for an incubated aqueous one in the absence (trace (2)) and presence of BTA (trace (3)). The as-mixed sample was prepared with a feed molar ratio of 2$CdCl_2$-8MPA-1SeU and with a $CdCl_2$ concentration of 10.0 mM for ESI-MS measurement. The incubated aqueous sample had a similar composition, and was stored at room temperature for 1.5 h first. The resulting sample was either kept further for additional 1.5 h, or extracted in a volume of 0.50 mL then mixed with BTA (1.50 mL) and water (1.00 mL) and kept for a duration of 1.5 h for ESI-MS measurement. The corresponding absorption spectra of these three samples are shown in Figs 2(b) and Fig. S7 in the ESM.

Both the as-mixed sample and incubated one without BTA were absorption featureless (Fig. 2(b), traces (1) and (2)). However, the former exhibited no characteristic signal in ESI-MS spectrum (Fig. 2(a), trace (1)), while the ESI-MS spectrum of the latter exhibited various characteristic signals that may be assigned to fragments with compositions of Cd_xSe_y (where x and y are integers) as labelled (Fig. 2(a), trace (2)). Upon mixing the incubated sample with BTA, CdSe MSC-420 formed (Fig. 2(b), trace (3)). The ESI-MS spectrum of the resulting mixture displayed also a series of Cd_xSe_y fragments (Fig. 2(a), trace (3)).

The ESI-MS signals obtained from the incubated sample (Fig. 2(a), trace (2)) suggest the formation of CdSe PCs with Cd–Se covalent bonds upon the hydrolysis of SeU in an alkaline aqueous solution [11, 16, 18]. The PCs fragmentized to result in Cd_xSe_y fragments during the ESI-MS measurement. The PCs then transformed to MSC-420 upon addition of BTA. Such a process is quite similar to the BTA-facilitated evolution from CdS PCs to

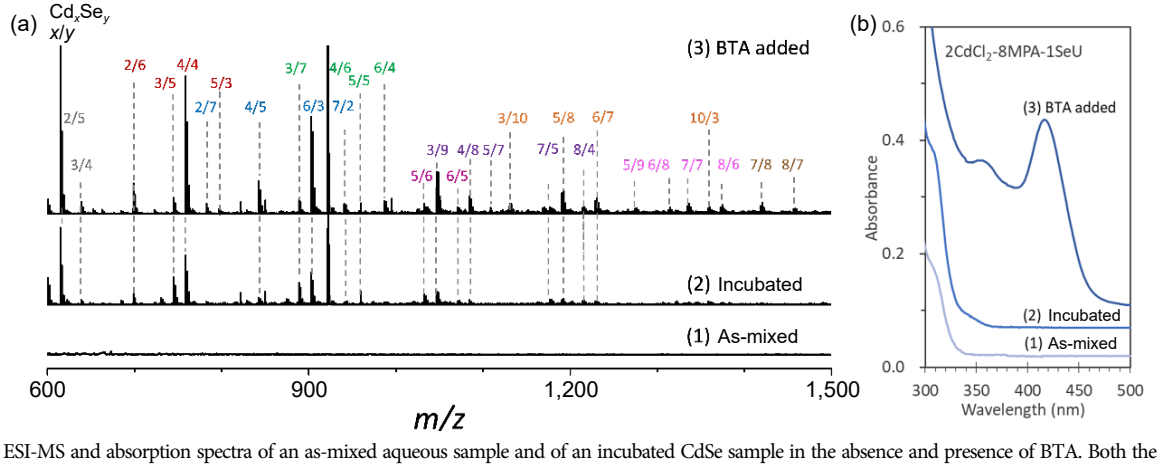

Figure 2 ESI-MS and absorption spectra of an as-mixed aqueous sample and of an incubated CdSe sample in the absence and presence of BTA. Both the as-mixed and incubated samples (pH about 12) had a feed molar ratio of 2$CdCl_2$-8MPA-1SeU with a $CdCl_2$ concentration of 10.0 mM. The as-mixed sample was prepared and measured for ESI-MS ((a), trace (1)) and absorption spectra ((b), trace (1)). One incubated sample was incubated at room temperature for 3.0 h for ESI-MS ((a), trace 2) and absorption measurements ((b), trace (2)). Another incubated sample was incubated at room temperature for 1.5 h first, and mixed with BTA and water and kept for additional 1.5 h for ESI-MS ((a), trace (3)) and absorption measurements ((b), trace (3)). The ESI-MS spectrometry investigations suggest the formation of CdSe PCs in the absorption featureless incubated sample.

CdS MSC-360 in aqueous solution [1]. The ESI-MS signals obtained from the sample with BTA (Fig. 2(a), trace (3)) are supposed to be relating to the fragmentation of CdSe MSC-420 during the ESI-MS measurements. It is noteworthy that a MSC and its corresponding PC are a pair of polymorphs with similar chemical compositions for the inorganic core [13], therefore, the ESI-MS spectra for samples containing PCs and/or MSCs exhibit quite similar signals.

3.3 The effect of Cd precursor on the formation of CdSe MSCs

To understand further the formation of CdSe MSC-420 from its counterpart PC in aqueous solutions, we investigated the interactions between Cd precursor and BTA, as well the self-assembling behavior of Cd precursors. Figure 3(a) shows the ^{1}H NMR spectra obtained from solutions of 80 mM BTA (trace (1)), 80 mM MPA and 200 mM KOH (trace (2)), and a mixture of 80 mM BTA, 80 mM MPA and 200 mM KOH in the presence of $CdCl_2$ with concentrations of 0.0 (trace (3)), 5.0 (trace (4)), 10.0 (trace (5)), 20.0 (trace (6)) and 40.0 mM (trace (7)). Figure 3(b) displays the proposed structures of Cd precursor with different ratios of $CdCl_2$ to MPA in the presence of BTA. Figure 3(c) presents the intensity ratio of the third (I_3, at about 380 nm) over the first (I_1, at about 370 nm) peaks (I_3/I_1) from pyrene (0.3 μM) emission spectra in alkaline solutions with $CdCl_2$ and MPA. These solutions had molar ratios of 1$CdCl_2$-2MPA (diamonds), 1$CdCl_2$-4MPA (triangles), 1$CdCl_2$-8MPA (squares), and 1$CdCl_2$-16MPA (circles). The solutions were stored under ambient conditions for 24 h before emission measurements with an excitation wavelength of 335 nm and with both excitation and emission silt widths of 2.5 nm.

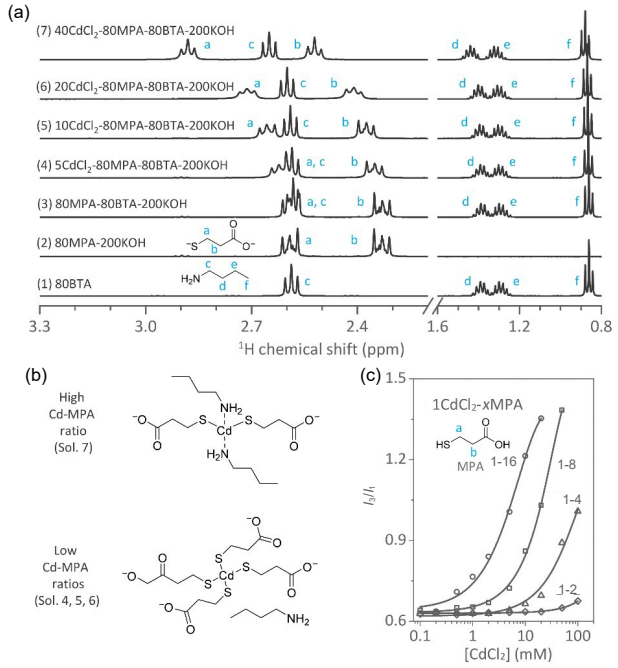

Figure 3 Investigations of the configurations and self-assemblies of Cd-MPA complexes with various $CdCl_2$ to MPA feed molar ratios. The configurations of Cd-MPA complexes were studied via ^{1}H NMR spectroscopy. The ^{1}H NMR spectra (a) were obtained from D_2O solutions of BTA (trace (1)), MPA and KOH (trace (2)), and a mixture of BTA, MPA and KOH in the presence of $CdCl_2$ with various concentrations (traces (3) to (7)). The possible configurations of Cd-MPA complexes with low ((b), bottom) and high $CdCl_2$-MPA feed molar ratios ((b), top) were proposed. The self-assemblies of Cd-MPA complexes were investigated in alkaline aqueous solutions with pyrene as a probe (c). The solutions had feed molar ratios of 1$CdCl_2$-2MPA (diamonds), 1$CdCl_2$-4MPA (triangles), 1$CdCl_2$-8MPA (squares), and 1$CdCl_2$-16MPA (circles). KOH was added to result in alkaline environments. The I_3/I_1 ratios were then extracted from all spectra obtained and were plotted with $CdCl_2$ concentration. Evidently, increasing the $CdCl_2$-MPA feed molar ratios facilitates the coordination of BTA with the Cd^{2+} capped with MPA, and inhibits the self-assembly of Cd-MPA complexes.

The ^{1}H NMR spectrum of BTA displayed four characteristic signals at 2.59, 1.38, 1.29, and 0.86 ppm (trace (1)), while that of MPA in the presence of KOH exhibited two resonance signals at 2.59 and 2.33 ppm (trace (2)). These ^{1}H resonance signals shifted little when BTA, MPA and KOH mixed together (trace (3)). For the resulting mixture, when $CdCl_2$ was added to have its concentration increasing from 5.0 to 20.0 mM, the two characteristic signals a and b of MPA shifted downfield gradually to 2.71 and 2.41 ppm, while those of BTA (c to f) changed little (traces (4) to (6)). Upon further increasing the $CdCl_2$ concentration to 40.0 mM, the signals a and b of MPA kept shifting downfield to 2.88 and 2.52 ppm, respectively, while the signal c relating to the α-proton of BTA shifted downfield significantly to 2.65 ppm as well (trace (7)).

It has been acknowledged that MPA coordinates with Cd^{2+} in alkaline aqueous solutions after the deprotonation of thiol group (Fig. S8 in the ESM) [1], and the binding constant between MPA and Cd^{2+} is much higher than that between primary amines (such as ETA and PrA) and Cd^{2+} [23]. According to the investigations of ^{1}H NMR spectroscopy, we proposed the corresponding configurations of Cd^{2+} with MPA and BTA (Fig. 3(b)). In the alkaline solutions with MPA and BTA, when the $CdCl_2$ concentration increased from 5.0 to 20.0 mM (with the $CdCl_2$-MPA ratios varying from 1-16 to 1-4), the Cd^{2+} prefers to bind with deprotonated MPA molecules (Fig. 3(b), bottom). The higher the Cd^{2+} concentration was, the more the MPA molecules were bonded. Further increasing the $CdCl_2$ concentration to 40.0 mM (with the $CdCl_2$-MPA ratio of 1-2) reduces significantly the amount of MPA molecules bonded with each Cd^{2+}, leading to empty positions on Cd^{2+} that are available for the coordination with primary amine groups (Fig. 3(b), top). As the CdSe PCs are generally regarded as Cd^{2+}-rich, we argue that the coordination between amine group with the Cd^{2+} of CdSe PCs may be responsible to the transformation from CdSe PCs to MSC-420.

It has been reported that the Cd-MPA complexes self-assemble in aqueous solutions to large aggregates with diameters more than 100 nm, and the resulting aggregates inhibit the formation of CdS MSC-360 [1]. However, the effect of $CdCl_2$-MPA feed molar ratios on the self-assembling behavior remains unknown. In the present work, the self-assembling behavior of the resulting Cd-MPA complexes in various molar ratios was investigated via fluorescence spectroscopy with pyrene as a probe. The I_3/I_1 ratio in the emission spectrum of pyrene increases significantly when pyrene molecules move from a polar environment to a relatively nonpolar one [43–46].

As demonstrated in Fig. 3(c), in solutions with 1$CdCl_2$-2MPA ratios (diamonds), when the $CdCl_2$ concentration was lower than 50.0 mM, the I_3/I_1 ratios obtained were quite similar to that obtained in deionized water (about 0.63). With 50.0 mM $CdCl_2$, the corresponding I_3/I_1 ratio increased to about 0.65, which increased to 0.68 with further increase of $CdCl_2$ concentration to 100.0 mM. Therefore, the aqueous solution of 1$CdCl_2$-2MPA exhibited a critical aggregation concentration (CAC) of about 50.0 mM (for $CdCl_2$). The CAC values decreased significantly to about 5.0, 2.0, and 0.5 mM in solutions with feed molar ratios of 1$CdCl_2$-4MPA (triangles), 1$CdCl_2$-8MPA (squares), and 1$CdCl_2$-16MPA (circles), respectively. Therefore, the presence of more MPA seems to facilitate the aggregation of the resulting Cd-MPA complexes. We noticed that the formation of CdSe MSC-420 in reaction batches of $CdCl_2$-MPA-SeU was inhibited significantly upon

decreasing the $CdCl_2$-MPA ratios with $CdCl_2$ in a constant concentration but MPA in various concentrations (Fig. S9 in the ESM). Such a result agrees well with the facilitated self-assembly of Cd-MPA complexes with lower $CdCl_2$-MPA ratios. We argue that the resulting aggregates encapsulate the CdSe PCs formed during incubation, which separate the PCs with the BTA molecules in the solution phase and inhibit their transformation to MSC-420.

3.4 Evolution of CdSe MSC-420 with Cys as the ligand

Cys has thiol, carboxyl, and primary amine groups, and it may be regarded as a combination of both MPA and BTA for the formation of CdSe MSC-420. Therefore, we argue that the formation of CdSe PCs and their transformation to CdSe MSCs occur simultaneously in aqueous reaction batches with Cys as a ligand in the absence of primary amines. Figure 4 shows the evolution of absorption spectra obtained from aqueous reaction batches (pH about 12.8) of $CdCl_2$-Cys-SeU with various $CdCl_2$-Cys feed molar ratios. The reaction mixtures had similar $CdCl_2$ and SeU concentrations of 10.0 and 5.0 mM, respectively, with the $CdCl_2$-Cys ratios of 1-2 (a), 1-4 (b), 1-8 (c), and 1-16 (d). After a certain reaction period, an aliquot (60 μL) of the resulting mixture was extracted and dispersed in 2.94 mL water for absorption measurement. Figure S10 in the ESM presents the absorption spectra obtained with various pH values.

As shown in Fig. 4, the absorption spectra of the $2CdCl_2$-4Cys-1SeU batch (a) showed a characteristic absorption peaking at around 380 nm with an intensity of 0.13 in a quite short period. Such a peak was gradually red-shifted to about 404 and 411 nm after 1 and 2 h, respectively, with the respective intensity increasing to 0.17 and 0.19. Afterwards, the peak kept red-shifting, with its absorbance increasing simultaneously. The peak appeared at 420 nm with an absorbance of about 0.61 after 72 h. The reaction batches of $2CdCl_2$-8Cys-1SeU and $2CdCl_2$-16Cys-1SeU were quite absorption featureless after dispersing, but exhibited a peak at about 420 nm after 1 h. Subsequently, the absorption peak position changed little, with its absorbance increasing gradually to 1.10 in 48 h and remaining unchanged up to 72 h. However, the absorbance for the peak at about 420 nm was only 0.26 for the batch of $2CdCl_2$-32Cys-1SeU after reacting for 72 h.

These absorption features suggest the formation of CdSe MSC-420 in the absence of CdSe QDs without additional primary amines. The $1CdCl_2$-4Cys and $1CdCl_2$-8Cys seemed to be the optimal feed molar ratios for the production of MSC-420. Batches with decreased or increased $CdCl_2$-Cys feed molar ratios seemed to inhibit the formation of CdSe MSC-420. Comparing to the batch with MPA and BTA, the use of Cys reduced significantly the amine group concentration for the formation of CdSe MSC-420. We argue that the passivation of the deprotonated thiol group with the Cd^{2+} of PCs may facilitate the interactions of the nearby amine group of Cys with PCs. Consequently, the CdSe PCs are more readily to transform to MSC-420. The resulting CdSe MSC-420 is quite stable in the reaction system. For example, in a reaction batch of $2CdCl_2$-8Cys-1SeU, the concentration of CdSe MSC-420 reached a plateau after reacting for 2 days, which changed little after a following duration up to 10 days (Fig. S10 in the ESM).

It is noteworthy that in the reaction batches of $2CdCl_2$-8Cys-1SeU, CdSe MSC-420 formed with pH ≥ 11.1, which was accelerated upon increasing the pH up to 12.9 but got inhibited by further increasing the pH to 14.0 (Fig. S11 in the ESM). The accelerated formation of MSC-420 in solutions with high pH values may be attributed to the facilitated hydrolysis of SeU, while the inhibited formation of MSC-420 at pH 14.0 may be due to the competitive formation of $Cd(OH)_2$ with a high OH^- concentration [27, 47]. Comparing the two processes of SeU hydrolysis and MSC-420 formation with various pH values (Fig. 1, and Figs. S1, S10 and S11 in the ESM), the SeU remained stable in solution with a pH of about 11.0 after 24 h (Fig. 1(d)), while MSC-420 evolved in a reaction batch with a similar condition (Fig. S11(a) in the ESM). We argue that the interaction of Cd-Cys complex with SeU promotes the hydrolysis of SeU, which is similar to the facilitated decomposition of thiourea in the presence of Cd-MPA complex [1]. As a side note, the formation of MSC-420 took a longer duration than the hydrolysis of SeU in solutions with pH from 12.0 to 14.0 (Fig. 1(f), and Figs. S1(a), S2(b), and S11(b)–S11(d) in the ESM). We therefore argue that the CdSe PCs formed in such a reaction system with a relatively faster rate than their

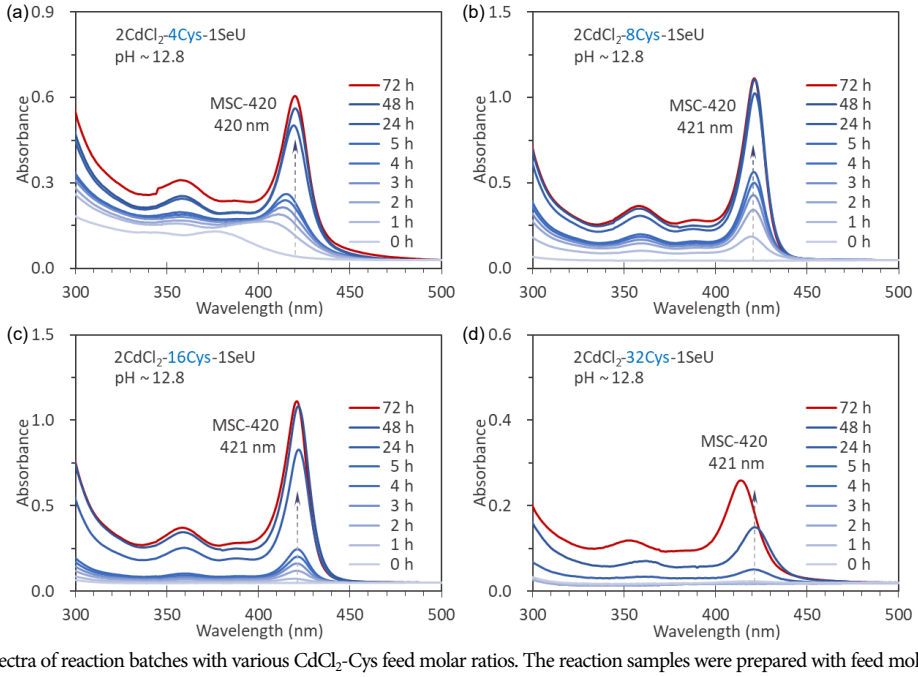

Figure 4 Absorption spectra of reaction batches with various $CdCl_2$-Cys feed molar ratios. The reaction samples were prepared with feed molar ratios of $2CdCl_2$-4Cys-1SeU (a), $2CdCl_2$-8Cys-1SeU (b), $2CdCl_2$-16Cys-1SeU (c), and $2CdCl_2$-32Cys-1SeU (d) in the presence of 10 mM $CdCl_2$. Similar to the reaction system with MPA, the presence of Cys in a too high concentration inhibits the eventual formation of CdSe MSC-420, which may due to the aggregation of Cd-Cys complexes. However, the batch of $1CdCl_2$-2Cys also shows the inhibited formation of CdSe MSC-420, which is different to the reaction system of MPA.

transformation to MSC-420. As the CdSe MSC-420 capped with Cys is able to be purified, we performed X-ray diffraction (XRD) measurement of the purified MSC-420 for its structural information. However, the XRD pattern exhibits quite broad signals (Fig. S12 in the ESM), which may be attributed to the limited atom number of MSC-420.

To further understand the inhibited formation of CdSe MSC-420 in reaction batches of $2CdCl_2$-4Cys-1SeU and $2CdCl_2$-32Cys-1SeU, we performed ^{1}H NMR and fluorescence experiments for the solutions with various $CdCl_2$-Cys feed molar ratios. Figure 5(a) presents the ^{1}H NMR spectra of D_2O solutions with 80.0 mM Cys (trace (1)), a mixture of 80.0 mM Cys and 200.0 mM KOH in the presence of $CdCl_2$ with concentrations of 0.0 (trace (2)), 5.0 (trace (3)), 10.0 (trace (4)), 20.0 (trace (5)), and 40.0 mM (trace (6)). We labeled the methylene (CH_2) proton at the same side with amine group as a_1 and the other one as a_2. The methenyl (CH) proton was labeled as b. Figure 5(b) displays the proposed configurations of Cd-Cys complexes with various feed molar ratios. Figure 5(c) presents the I_3/I_1 ratios of pyrene (0.3 μM) from four alkaline aqueous mixtures with ratios of $1CdCl_2$-2Cys (diamonds), $1CdCl_2$-4Cys (triangles), $1CdCl_2$-8Cys (squares), and $1CdCl_2$-16Cys (circles).

The ^{1}H NMR spectrum of the Cys solution (pH about 5.8) exhibited three resonance signals centered at about 3.02, 3.11, and 3.99 ppm (trace (1)), which were corresponding to the protons a_1, a_2, and b, respectively, according to their coupling constants (Table S1 in the ESM). In the solution with 80 mM Cys and 200 mM KOH (pH about 12.1), the characteristic signals of Cys shifted upfield to 2.46, 2.90, and 3.09 ppm (trace (2)), which may be assigned to protons a_1, a_2 and b according to the HSQC pattern (Fig. S13 in the ESM) and the coupling constant of each signal (Table S1 in the ESM). After the deprotonation of carboxyl, thiol, and amine groups with the respective pK_a values of 1.92, 8.37, and 10.70, the electronic repulsion between the negatively charged deprotonated carboxyl and thiol groups restricted the rotation of C–C bonds. Therefore, the chirality of the carbon atom bonded with amine group led to the significant difference of the chemical shift of signals for protons a_1 and a_2. In the presence of 5.0 and 10.0 mM $CdCl_2$ (traces (3) and (4), respectively), the three characteristic signals for deprotonated Cys shifted downfield slightly. Upon increasing the $CdCl_2$ concentration to 20.0 mM, the signals for protons a_1, a_2 and b were at 2.59, 2.92, and 3.25 ppm, respectively (trace (5)). Further increasing the $CdCl_2$ concentration to 40.0 mM, the signals of protons a_1, a_2, and b shifted downfield to 2.77, 2.97, and 3.48 ppm, respectively (trace (6)).

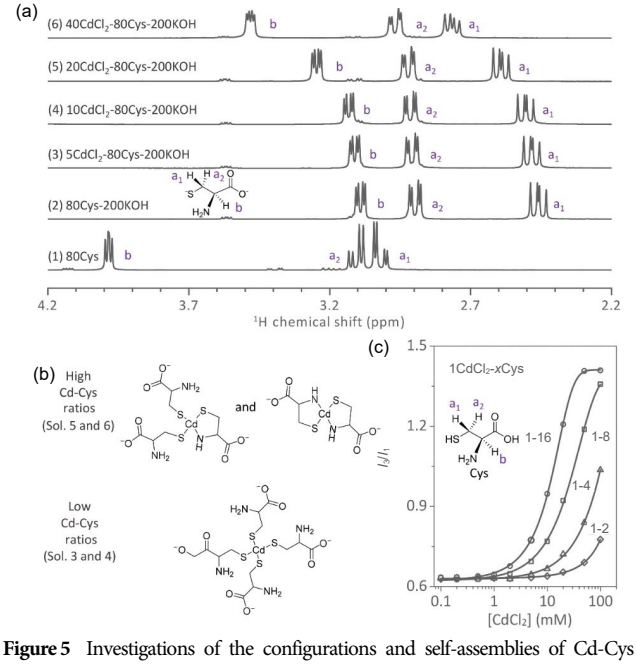

Figure 5 Investigations of the configurations and self-assemblies of Cd-Cys complexes with various $CdCl_2$ to Cys feed molar ratios. The configurations of Cd-Cys complexes were studied via ^{1}H NMR spectroscopy. The ^{1}H NMR spectra (a) were obtained from D_2O solutions with Cys (trace (1)), a mixture of Cys and KOH in the presence of $CdCl_2$ with various concentrations (traces (2) to (6)). The possible configurations of Cd-Cys complexes with low ((b), bottom) or high $CdCl_2$-Cys feed molar ratios ((b), top) were proposed. The self-assemblies of Cd-Cys complexes were investigated in alkaline aqueous solutions with pyrene as a probe (c). The solutions had feed molar ratios of $1CdCl_2$-2Cys (diamonds), $1CdCl_2$-4Cys (triangles), $1CdCl_2$-8Cys (squares), and $1CdCl_2$-16Cys (circles). KOH was added to result in alkaline environments. The I_3/I_1 ratios then extracted from all spectra obtained and were plotted with $CdCl_2$ concentration. Evidently, increasing the $CdCl_2$-Cys feed molar ratios facilitates the formation of Cd-Cys complex in a partially closed configuration with both thiol and primary amine groups on Cys coordinated with Cd^{2+}. In addition, increasing the $CdCl_2$-Cys feed molar ratios also inhibits the self-assembly of Cd-Cys complexes, which is similar to the solutions with MPA.

Comparing the chemical shifts of three characteristic signals, the signal a_2 exhibited limited downfield shifts by increasing the $CdCl_2$ concentrations. The downfield shifts of signals a_1 and b were quite small in solutions with $1CdCl_2$-16Cys and $1CdCl_2$-8Cys ratios (traces (3) and (4)), but became significant in solutions with $1CdCl_2$-4Cys and $1CdCl_2$-2Cys ratios (traces (5) and (6)). As protons a_1 and b are spatially close to the amine group in Cys, their significant change in chemical shift upon increasing the $CdCl_2$-Cys ratio seems to be attributed to the coordination of amine group with Cd^{2+}.

Therefore, we proposed that with low $CdCl_2$-Cys feed molar ratios, the Cys molecules bonded with Cd^{2+} via the deprotonated thiol group (Fig. 5(b), bottom), whereas the amine group involved in the coordination with high $CdCl_2$-Cys feed molar ratios due to the lack of enough thiol groups (Fig. 5(b), top). Upon increasing $CdCl_2$ concentration (traces (3) to (6)), the configuration of Cd-Cys complex might change from $[Cd(Cys)_4]^{6-}$ to $[Cd(Cys)_3]^{4-}$ and then to $[Cd(Cys)_2]^{2-}$ (Fig. S14 in the ESM). Such a result agrees well with the configurations of Cd-Cys complexes proposed in literature via different techniques such as ^{113}Cd NMR spectroscopy [48]. The DFT calculation indicated that $[Cd(Cys)_2]^{2-}$ complex with both thiol and amine groups coordinated with Cd^{2+} was more stable than that with only thiol groups coordinated (Fig. S15 in the ESM). In the $[Cd(Cys)_2]^{2-}$ complex, the centered Cd^{2+} appeared to be clawed by two Cys molecules. Such a configuration shields the Cd^{2+} from the outer aqueous environment and reduces the collision possibility with Se^{2-} derived from SeU. Consequently, the reactivity of Cd precursor towards the formation of CdSe PCs and MSC-420 was reduced significantly (Fig. 4(a)).

As demonstrated in Fig. 5(c), for the alkaline aqueous solutions of $CdCl_2$ and Cys, the CAC (for $CdCl_2$) obtained from the solutions of $1CdCl_2$-2Cys was as high as 20.0 mM, which decreased to about 10.0, 5.0, and 2.0 mM in aqueous solutions with feed molar ratios of $1CdCl_2$-4Cys, $1CdCl_2$-8Cys, and $1CdCl_2$-16Cys, respectively. Similar to the reaction batches with MPA and BTA, the aggregation of Cd-Cys complexes inhibited significantly the formation of CdSe MSC-420 (Fig. S16 in the ESM). Therefore, the inhibited formation of CdSe MSC-420 in the reaction batch of $2CdCl_2$-32Cys-1SeU with 10.0 mM $CdCl_2$ (Fig. 4(d)) was attributed to the aggregation of Cd-Cys complexes.

4 Conclusion

In conclusion, we have developed a PC-enabled formation pathway of aqueous CdSe MSC-420 at room temperature. The aqueous-phase CdSe MSC-420 was synthesized by using $CdCl_2$ and SeU as the respective Cd and Se sources, and MPA as the

ligand. The first step was the formation of CdSe PCs in the alkaline aqueous solutions upon the hydrolysis of SeU, while the second step involved the transformation from CdSe PCs to MSC-420 upon the addition of a primary amine such as BTA. ESI-MS measurements suggest the presence of species with Cd-Se covalent bonds in the absorption featureless sample obtained after the first step of the reaction, supporting the formation of CdSe PCs. The ^{1}H NMR spectra of solutions with various $CdCl_2$-MPA feed molar ratios suggest the interaction of primary amine group and Cd^{2+}, which may be responsible to the transformation from PCs to MSCs. The Cd-MPA complex self-assembles in aqueous solutions when its concentration is above the CAC. The lower the molar ratio of $CdCl_2$ to MPA, the lower the CAC for the corresponding Cd-MPA complex. The resulting aggregates may encapsulate CdSe PCs and isolate them with the primary amines in the solution phase, which inhibit their transformation to MSC-420. Therefore, in reaction batches of $CdCl_2$-MPA-SeU with similar $CdCl_2$ and SeU concentrations, increasing the MPA concentration may result in the inhibited formation of CdSe MSC-420. When Cys, which has both thiol and amine groups, is used as a ligand, CdSe MSC-420 forms directly in the absence of additional primary amines. In such a reaction system, the formation of PCs and their transformation to MSC-420 occur simultaneously. With 10.0 mM $CdCl_2$, the formation of CdSe MSC-420 is favored in batches of $2CdCl_2$-8Cys-1SeU and $2CdCl_2$-16Cys-1SeU, but gets inhibited significantly in reaction batches of $2CdCl_2$-4Cys-1SeU and $2CdCl_2$-32Cys-1SeU. ^{1}H NMR spectroscopy suggests that with high $CdCl_2$-Cys feed molar ratios, the amine group on Cys coordinates with Cd^{2+}. The resulting Cd-Cys complex exhibits a partially closed configuration, which inhibits its further covalent bonding with Se^{2-} derived from SeU, resulting in the inhibited formation of MSC-420. The Cd-Cys complexes also self-assemble in aqueous solutions, which is facilitated upon decreasing the $CdCl_2$-Cys feed molar ratios. Therefore, the inhibited formation of CdSe MSC-420 with a quite low $CdCl_2$-Cys feed molar ratio is due to the facilitated aggregation of the Cd-Cys complexes. The present study provides an in-depth understanding towards the formation pathway of aqueous-phase CdSe MSC-420. These investigations may guide the synthesis of aqueous-phase semiconductor MSCs with different compositions and may promote the synthesis of aqueous-phase semiconductor nanocrystals from an empirical art to science.

Acknowledgements

K. Y. thanks the National Natural Science Foundation of China (No. 21773162), the Fundamental Research Funds for the Central Universities, the Applied Basic Research Programs of Science and Technology Department of Sichuan Province (No. 2020YJ0326), the State Key Laboratory of Polymer Materials Engineering of Sichuan University (No. sklpme2020-2-09), the Open Project of Key State Laboratory for Supramolecular Structures and Materials of Jilin University (No. SKLSSM 2021030), and the National Major Scientific and Technological Special Project for "Significant New Drugs Development" (No. 2019ZX09201005-005-002). M. Z. is grateful to the National Natural Science Foundation of China (No. 22002099), China Postdoctoral Science Foundation (No. 2020T130441), Sichuan University postdoctoral interdisciplinary Innovation Fund, and the Open Project of Key State Laboratory for Supramolecular Structures and Materials of Jilin University (No. SKLSSM 2021032). We would like to thank the Analytical & Testing Center of Sichuan University for both ESI-MS and NMR measurements.

Electronic Supplementary Material: Supplementary material (additional optical absorption spectra, HSQC spectra and DFT calculations (PDF)) is available in the online version of this article at https://doi.org/10.1007/s12274-021-3858-1.

References

[1] Wan, W. S.; Zhang, M.; Zhao, M.; Rowell, N.; Zhang, C. C.; Wang, S. L.; Kreouzis, T.; Fan, H. S.; Huang, W.; Yu, K. Room-temperature formation of CdS magic-size clusters in aqueous solutions assisted by primary amines. *Nat. Commun.* **2020**, *11*, 4199.

[2] He, L.; Luan, C. R.; Rowell, N.; Zhang, M.; Chen, X. Q.; Yu, K. Transformations among colloidal semiconductor magic-size clusters. *Acc. Chem. Res.* **2021**, *54*, 776–786.

[3] Zhu, J. M.; Cao, Z. P.; Zhu, Y. C.; Rowell, N.; Li, Y.; Wang, S. L.; Zhang, C. C.; Jiang, G.; Zhang, M.; Zeng, J. R. et al. Transformation pathway from CdSe magic-size clusters with absorption doublets at 373/393 nm to clusters at 434/460 nm. *Angew. Chem., Int. Ed.* **2021**, *60*, 20358–20365.

[4] Yang, X. X.; Zhang, M.; Shen, Q.; Li, Y.; Luan, C. R.; Yu, K. The precursor compound of two types of ZnSe magic-sized clusters. *Nano Res*., in press, https://doi.org/10.1007/s12274-021-3503-z.

[5] Shen, Q.; Luan, C. R.; Rowell, N.; Zhang, M.; Wang, K.; Willis, M.; Chen, X. Q.; Yu, K. Reversible transformations at room temperature among three types of CdTe magic-size clusters. *Inorg. Chem.* **2021**, *60*, 4243–4251.

[6] Palencia, C.; Yu, K.; Boldt, K. The future of colloidal semiconductor magic-size clusters. *ACS Nano* **2020**, *14*, 1227–1235.

[7] Zhang, H.; Luan, C. R.; Gao, D.; Zhang, M.; Rowell, N.; Willis, M.; Chen, M.; Zeng, J. R.; Fan, H. S.; Huang, W. et al. Room-temperature formation pathway for CdTeSe alloy magic-size clusters. *Angew. Chem., Int. Ed.* **2020**, *59*, 16943–16952.

[8] Chen, M.; Luan, C. R.; Zhang, M.; Rowell, N.; Willis, M.; Zhang, C. C.; Wang, S. L.; Zhu, X. H.; Fan, H. S.; Huang, W. et al. Evolution of CdTe magic-size clusters with single absorption doublet assisted by adding small molecules during prenucleation. *J. Phys. Chem. Lett.* **2020**, *11*, 2230–2240.

[9] Li, L. J.; Zhang, J.; Zhang, M.; Rowell, N.; Zhang, C. C.; Wang, S. L.; Lu, J.; Fan, H. S.; Huang, W.; Chen, X. Q. et al. Fragmentation of magic-size cluster precursor compounds into ultrasmall CdS quantum dots with enhanced particle yield at low temperatures. *Angew. Chem., Int. Ed.* **2020**, *59*, 12013–12021.

[10] Liu, S. P.; Yu, Q. Y.; Zhang, C. C.; Zhang, M.; Rowell, N.; Fan, H. S.; Huang, W.; Yu, K.; Liang, B. Transformation of ZnS precursor compounds to magic-size clusters exhibiting optical absorption peaking at 269 nm. *J. Phys. Chem. Lett.* **2020**, *11*, 75–82.

[11] Gao, D.; Hao, X. Y.; Rowell, N.; Kreouzis, T.; Lockwood, D. J.; Han, S.; Fan, H. S.; Zhang, H.; Zhang, C. C.; Jiang, Y. N. et al. Formation of colloidal alloy semiconductor CdTeSe magic-size clusters at room temperature. *Nat. Commun.* **2019**, *10*, 1674.

[12] Zhang, J.; Hao, X. Y.; Rowell, N.; Kreouzis, T.; Han, S.; Fan, H. S.; Zhang, C. C.; Hu, C. W.; Zhang, M.; Yu, K. Individual pathways in the formation of magic-size clusters and conventional quantum dots. *J. Phys. Chem. Lett.* **2018**, *9*, 3660–3666.

[13] Luan, C. R.; Tang, J. B.; Rowell, N.; Zhang, M.; Huang, W.; Fan, H. S.; Yu, K. Four types of CdTe magic-size clusters from one prenucleation stage sample at room temperature. *J. Phys. Chem. Lett.* **2019**, *10*, 4345–4353.

[14] Luan, C.; Gökçinar, Ö. Ö.; Rowell, N.; Kreouzis, T.; Han, S.; Zhang, M.; Fan, H. S.; Yu, K. Evolution of two types of CdTe magic-size clusters from a single induction period sample. *J. Phys. Chem. Lett.* **2018**, *9*, 5288–5295.

[15] Wang, L. X.; Hui, J.; Tang, J. B.; Rowell, N.; Zhang, B. W.; Zhu, T. T.; Zhang, M.; Hao, X. Y.; Fan, H. S.; Zeng, J. R. et al. Precursor self-assembly identified as a general pathway for colloidal semiconductor magic-size clusters. *Adv. Sci.* **2018**, *5*, 1800632.

[16] Zhu, D. K.; Hui, J.; Rowell, N.; Liu, Y. Y.; Chen, Q. Y.; Steegemans, T.; Fan, H. S.; Zhang, M.; Yu, K. Interpreting the ultraviolet absorption in the spectrum of 415 nm-bandgap CdSe magic-size clusters. *J. Phys. Chem. Lett.* **2018**, *9*, 2818–2824.

[17] Zhu, T. T.; Zhang, B. W.; Zhang, J.; Lu, J.; Fan, H. S.; Rowell, N.; Ripmeester, J. A.; Han, S.; Yu, K. Two-step nucleation of CdS magic-size nanocluster MSC-311. *Chem. Mater.* **2017**, *29*, 5727–5735.
[18] Liu, M. Y.; Wang, K.; Wang, L. X.; Han, S.; Fan, H. S.; Rowell, N.; Ripmeester, J. A.; Renoud, R.; Bian, F. G.; Zeng, J. R. et al. Probing intermediates of the induction period prior to nucleation and growth of semiconductor quantum dots. *Nat. Commun.* **2017**, *8*, 15467.
[19] Zhang, J.; Li, L. J.; Rowell, N.; Kreouzis, T.; Willis, M.; Fan, H. S.; Zhang, C. C.; Huang, W.; Zhang, M.; Yu, K. One-step approach to single-ensemble CdS magic-size clusters with enhanced production yields. *J. Phys. Chem. Lett.* **2019**, *10*, 2725–2732.
[20] Zhang, B. W.; Zhu, T. T.; Ou, M. Y.; Rowell, N.; Fan, H. S.; Han, J. T.; Tan, L.; Dove, M. T.; Ren, Y.; Zuo, X. B. et al. Thermally-induced reversible structural isomerization in colloidal semiconductor CdS magic-size clusters. *Nat. Commun.* **2018**, *9*, 2499.
[21] Liu, Z. M.; Shao, C. Y.; Jin, B.; Zhang, Z. S.; Zhao, Y. Q.; Xu, X. R.; Tang, R. K. Crosslinking ionic oligomers as conformable precursors to calcium carbonate. *Nature* **2019**, *574*, 394–398.
[22] Dey, A.; Bomans, P. H. H.; Müller, F. A.; Will, J.; Frederik, P. M.; de With, G.; Sommerdijk, N. A. J. M. The role of prenucleation clusters in surface-induced calcium phosphate crystallization. *Nat. Mater.* **2010**, *9*, 1010–1014.
[23] Han, J. S.; Luo, X. T.; Zhou, D.; Sun, H. Z.; Zhang, H.; Yang, B. Growth kinetics of aqueous CdTe nanocrystals in the presence of simple amines. *J. Phys. Chem. C* **2010**, *114*, 6418–6425.
[24] Zhou, D.; Lin, M.; Chen, Z. L.; Sun, H. Z.; Zhang, H.; Sun, H. C.; Yang, B. Simple synthesis of highly luminescent water-soluble CdTe quantum dots with controllable surface functionality. *Chem. Mater.* **2011**, *23*, 4857–4862.
[25] Lesnyak, V.; Gaponik, N.; Eychmuller, A. Colloidal semiconductor nanocrystals: The aqueous approach. *Chem. Soc. Rev.* **2013**, *42*, 2905–2929.
[26] Zhou, D.; Liu, M.; Lin, M.; Bu, X. Y.; Luo, X. T.; Zhang, H.; Yang, B. Hydrazine-mediated construction of nanocrystal self-assembly materials. *ACS Nano* **2014**, *8*, 10569–10581.
[27] Jing, L. H.; Kershaw, S. V.; Li, Y. L.; Huang, X. D.; Li, Y. Y.; Rogach, A. L.; Gao, M. Y. Aqueous based semiconductor nanocrystals. *Chem. Rev.* **2016**, *116*, 10623–10730.
[28] Yao, D.; Liu, Y.; Li, J.; Zhang, H. Advances in green colloidal synthesis of metal selenide and telluride quantum dots. *Chin. Chem. Lett.* **2019**, *30*, 277–284.
[29] Aires, A.; Möller, M.; Cortajarena, A. L. Protein design for the synthesis and stabilization of highly fluorescent quantum dots. *Chem. Mater.* **2020**, *32*, 5729–5738.
[30] Mrad, M.; Ben Chaabane, T.; Rinnert, H.; Lavinia, B.; Jasniewski, J.; Medjahdi, G.; Schneider, R. Aqueous synthesis for highly emissive 3-mercaptopropionic acid-capped AIZS quantum dots. *Inorg. Chem.* **2020**, *59*, 6220–6231.
[31] Park, Y. S.; Dmytruk, A.; Dmitruk, I.; Kasuya, A.; Okamoto, Y.; Kaji, N.; Tokeshi, M.; Baba, Y. Aqueous phase synthesized CdSe nanoparticles with well-defined numbers of constituent atoms. *J. Phys. Chem. C* **2010**, *114*, 18834–18840.
[32] Park, Y. S.; Dmytruk, A.; Dmitruk, I.; Kasuya, A.; Takeda, M.; Ohuchi, N.; Okamoto, Y.; Kaji, N.; Tokeshi, M.; Baba, Y. Size-selective growth and stabilization of small CdSe nanoparticles in aqueous solution. *ACS Nano* **2010**, *4*, 121–128.
[33] Kurihara, T.; Matano, A.; Noda, Y.; Takegoshi, K. Rotational motion of ligand-cysteine on CdSe magic-sized clusters. *J. Phys. Chem. C* **2019**, *123*, 14993–14998.
[34] Baker, J. S.; Nevins, J. S.; Coughlin, K. M.; Colón, L. A.; Watson, D. F. Influence of complex-formation equilibria on the temporal persistence of cysteinate-functionalized CdSe nanocrystals in water. *Chem. Mater.* **2011**, *23*, 3546–3555.
[35] Kurihara, T.; Noda, Y.; Takegoshi, K. Quantitative solid-state NMR study on ligand-surface interaction in cysteine-capped CdSe magic-sized clusters. *J. Phys. Chem. Lett.* **2017**, *8*, 2555–2559.
[36] Kurihara, T.; Noda, Y.; Takegoshi, K. Capping structure of ligand-cysteine on CdSe magic-sized clusters. *ACS Omega* **2019**, *4*, 3476–3483.
[37] Zhao, Y.; Truhlar, D. G. The M06 suite of density functionals for main group thermochemistry, thermochemical kinetics, noncovalent interactions, excited states, and transition elements: Two new functionals and systematic testing of four M06-class functionals and 12 other functionals. *Theor. Chem. Acc.* **2008**, *120*, 215–241.
[38] Cammi, R.; Mennucci, B.; Tomasi, J. Fast evaluation of geometries and properties of excited molecules in solution: A Tamm-Dancoff model with application to 4-dimethylaminobenzonitrile. *J. Phys. Chem. A* **2000**, *104*, 5631–5637.
[39] Marenich, A. V.; Cramer, C. J.; Truhlar, D. G. Uniform treatment of solute-solvent dispersion in the ground and excited electronic states of the solute based on a solvation model with state-specific polarizability. *J. Chem. Theory Comput.* **2013**, *9*, 3649–3659.
[40] Wang, C. L.; Zhang, H.; Zhang, J. H.; Lv, N.; Li, M. J.; Sun, H. Z.; Yang, B. Ligand dynamics of aqueous CdTe nanocrystals at room temperature. *J. Phys. Chem. C* **2008**, *112*, 6330–6336.
[41] Wurmbrand, D.; Fischer, J. W. A.; Rosenberg, R.; Boldt, K. Morphogenesis of anisotropic nanoparticles: Self-templating via non-classical, fibrillar Cd_2Se intermediates. *Chem. Commun.* **2018**, *54*, 7358–7361.
[42] Kirkwood, N.; Boldt, K. Protic additives determine the pathway of CdSe nanocrystal growth. *Nanoscale* **2018**, *10*, 18238–18248.
[43] Zhang, M.; Fives, C.; Waldron, K. C.; Zhu, X. X. Self-assembly of a bile acid dimer in aqueous solutions: From nanofibers to nematic hydrogels. *Langmuir* **2017**, *33*, 1084–1089.
[44] Zhang, M.; Ma, Z. Y.; Wang, K. J.; Zhu, X. X. CO_2 sequestration by bile salt aqueous solutions and formation of supramolecular hydrogels. *ACS Sustainable Chem. Eng.* **2019**, *7*, 3949–3955.
[45] Chen, Y. L.; Luo, J. T.; Zhu, X. X. Fluorescence study of inclusion complexes between star-shaped cholic acid derivatives and polycyclic aromatic fluorescent probes and the size effects of host and guest molecules. *J. Phys. Chem. B* **2008**, *112*, 3402–3409.
[46] Luo, J. T.; Chen, Y. L.; Zhu, X. X. Invertible amphiphilic molecular pockets made of cholic acid. *Langmuir* **2009**, *25*, 10913–10917.
[47] Shavel, A.; Gaponik, N.; Eychmüller, A. Factors governing the quality of aqueous CdTe nanocrystals: Calculations and experiment. *J. Phys. Chem. B* **2006**, *110*, 19280–19284.
[48] Jalilehvand, F.; Leung, B. O.; Mah, V. Cadmium(II) complex formation with cysteine and penicillamine. *Inorg. Chem.* **2009**, *48*, 5758–5771.